*Carbohydrate Research*, 247 (1993) 51–62
Elsevier Science Publishers B.V., Amsterdam



# Computer modeling of the tetrasaccharide nystose

Alfred D. French [a], Nadine Mouhous-Riou [b] and Serge Pérez [b]

[a] *Southern Regional Research Center, New Orleans, Louisiana 70179 (USA)*
[b] *Institut Nationale de la Recherche Agronomique, F-44026 Nantes (France)*

(Received September 18th, 1992; accepted in revised form March 9th, 1993)

## ABSTRACT

Nystose, *O*-β-D-fructofuranosyl-(2 → 1)-*O*-β-D-fructofuranosyl-(2 → 1)-β-D-fructofuranosyl α-D-glucopyranoside, was modeled with the rigid-residue program PFOS and with MM3. The three furanose rings of crystalline nystose trihydrate all are within the 1 kcal·mol$^{-1}$ contour on an MM3 energy surface that was calculated with a dielectric constant of 4. The calculations showed that in the extended conformation found in the crystal, there was a small influence of the remainder of the residues on the conformation of any given disaccharide segment. Even accounting for intramolecular, interresidue forces, however, the central inulobiose and the sucrose linkages appear to be distorted. These discrepancies are apparently due to crystal packing forces and, for the sucrose linkage, miscalculation of the energy of an overlapping exoanomeric effect, as indicated by studies of a model miniature crystal. The different conformations of the central and terminal inulobiose linkages in the crystal show that conformations in higher oligosaccharides will not always correspond to the global minima on conformational maps for isolated disaccharides.

## INTRODUCTION

Nystose, *O*-β-D-fructofuranosyl-(2 → 1)-*O*-β-D-fructofuranosyl-(2 → 1)-β-D-fructofuranosyl α-D-glucopyranoside (Chart 1) is found in mixtures of similar nonreducing oligosaccharides and inulin-type polysaccharides called fructans. Crystals of its trihydrate were grown in Nantes and the crystal structure was determined by Jeffrey and Huang as described in the immediately preceding paper[1]. Crystal structures of two of its subunits (Chart 1) were determined previously: sucrose[2,3] and 1-kestose[4]. The crystal structures of two related oligosaccharides have also been reported: cycloinulohexaose[5], and 6-kestose (β-D-Fru*f*-(2 → 6)-β-D-Fru*f*-(2 ↔ 1)-α-D-Glc*p*[6]. Nystose and stachyose[7], which have several features in common, are the only tetrasaccharides for which crystals have been grown and successfully analyzed by diffraction. Both contain sucrose moieties, are nonreducing and have two three-bond linkages. The availability of a crystal

Nystose

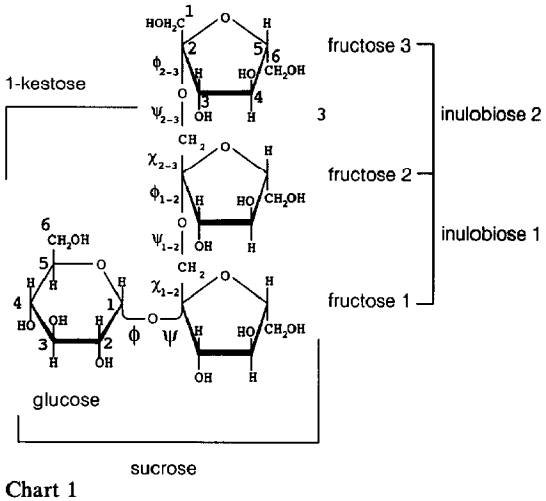


Chart 1

structure for nystose thus gives a rare opportunity to compare model oligosaccharides with diffraction results.

Nystose is more difficult to model than most tetrasaccharides. Detailed simultaneous study of all eight interresidue linkage bonds alone would be overwhelming. Nystose also has three flexible furanose rings, five rotating primary alcohol groups and 14 rotating hydroxyl groups, all of which are important in energy calculations. Conformational energies of the β-D-fructofuranose subunit were obtained earlier[8], and sucrose has been studied several times[6,9–11]. Inulobiose (Chart 1) has been modeled with both fructose rings in the furanose form[12]. Analysis of 1-kestose by modeling and NMR[13] suggested that the unusual puckering of the central fructofuranose ring found in crystals of 1-kestose resulted from crystallization, and that it was not inherent in the β-D-Fru*f*-(1 → 1)-β-D-Fru*f*-(2 ↔ 1)-α-D-Glc*p* sequence.

In our analysis of nystose, we used both PFOS, a traditional, rigid-residue program for computer modeling, and MM3, a versatile program that permits study of structures with full relaxation of the geometric features during energy minimization. PFOS permitted rapid scanning of variation space for the disaccharide linkages, even when all four sugar residues of the tetrasaccharide were included. MM3 was used for the modeling tasks that are beyond the scope of the PFOS program, including a new analysis of fructofuranose rings and minimization studies of nystose. Both an isolated nystose molecule and a miniature crystal model were minimized. PFOS and MM3 were used in parallel to analyze sucrose for comparative purposes and to learn whether the ability of MM3 to allow the residues to relax would better rationalize the set of sucrosyl linkage conformations observed in various crystal structure studies.

## CALCULATIONS

The PFOS and MM3 programs are briefly described in the Appendix. Fructofuranose envelope (*E*), symmetrical twist (*T*), and nonsymmetrical twist (intermediate) conformations were studied with MM3. Starting with a planar fructofuranose ring and a local program, 720 individual conformations were generated by 0.1 Å movements of single and coupled movements of adjacent ring atoms (with their substituents) over ranges of ±0.8 Å perpendicular to the plane. Each ring conformation was examined with nine combinations of the three staggered orientations of the two primary alcohol groups. These somewhat distorted structures were optimized, with the out-of-plane ring atoms held at their initial distances from the plane. The lowest of the nine energies calculated at each of the 720 points was used to construct the map shown in Fig. 1. The Cremer–Pople[14,15] puckering phase angles ($\Phi$) and amplitudes ($q$) were converted to clockwise Cartesian values before plotting.

MM3 studies of the sucrosyl linkage used the approach described earlier for disaccharides[16], with four starting models and 20° increments of rotations for the torsion angles O-5–C-1–O-1–C-2′ ($\phi$) and O-2′–C-2′–O-1–C-1 ($\psi$). For the region $\phi = 40$ to 120° and $\psi = -100$ to 20° that encompasses crystal structures containing sucrose-type linkages, 16 starting geometries were used, including *gt* and *gg* positions of C-6–O-6 and clockwise and reverse clockwise[16] hydroxyl groups on the glucose residue. Starting models also incorporated variations of the fructose unit, with two orientations each of the C-1′–O-1′ (*gg* and *tg*) and C-6′–O-6′ (*gt* and *gg*) bonds. (The first letter denotes the *gauche* or *trans* relationship with the ring oxygen, and, for the furanose rings, the second letter specifies the relationship with C-3 and C-4, respectively.) The lowest energy, regardless of starting model, was selected at each $\phi$, $\psi$ point to prepare the maps shown in Fig. 2.

PFOS energy maps were calculated for the sucrose residue and for both inulobiosyl linkages. PFOS allows simultaneous variation of only two torsion angles of adjacent bonds. Therefore, the third bond of the inulobiose linkages retained the geometry found in the crystal structure. Increments of rotation about the bonds were 5°. The starting models were all based on the nystose crystal structure, with C–H bond lengths increased to 1.09 Å.

In the first set of inulobiose maps, shown in Fig. 3, the two torsion angles varied were $\phi_{1-2}$ (O-2″–C-2″–O-1′–C-1′) or $\phi_{2-3}$ (O-2‴–C-2‴–O-1″–C-1″) and $\psi_{1-2}$ (C-2″–O-1′–C-1′–C-2′) or $\psi_{2-3}$ (C-2‴–O-1″–C-1″–C-2″). In a second set of maps (not shown), the values of $\psi_{1-2}$ and $\psi_{2-3}$ were varied, along with $\chi_{1-2}$ (O-2′–C-2′–C-1′–O-1′) or $\chi_{2-3}$ (O-2″–C-2″–C-1″–O-1″).

To check for intramolecular reasons for distortions of the various disaccharide linkages, the complete nystose molecule was modeled by optimizing the entire molecule with MM3 in isolation, starting with the coordinates from the crystal structure. To learn whether apparent distortions arise from intermolecular forces,

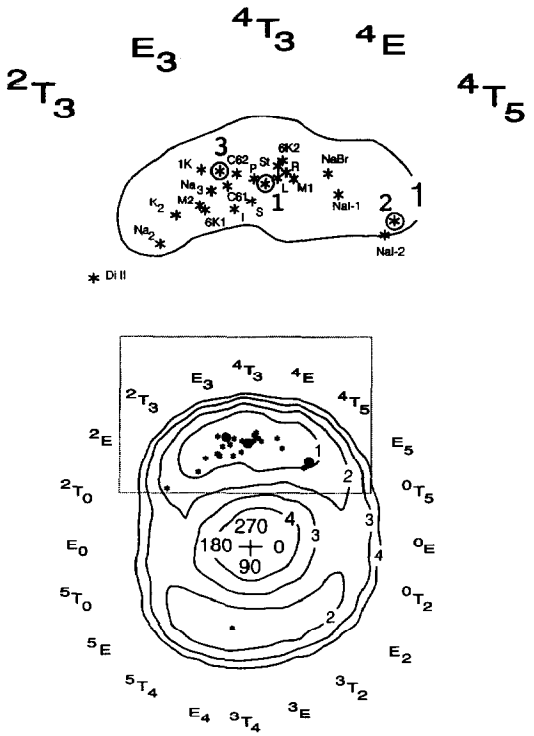


Fig. 1. Puckering energies of isolated β-D-fructofuranose in kcal·mol$^{-1}$ calculated with MM3. The lower part of the figure shows all possible structures and the gray box encloses the northern region where most crystallographically determined fructose rings are found. The $E$ and $T$ notation surrounds the figure, and the Cremer–Pople phase ($\Phi$) is indicated by the numbers at the center. Points shown as asterisks represent crystallographically determined puckering values; those circled are from the present determination of nystose. The sole point in the Southern region, near $E_4$, is from 1-ketose[4]. The upper part of the figure is an enlargement of the area enclosed by the box in the lower part of the figure. Points in the northern region are (from left to right): Di II, difructose dianhydride II[32]; $Na_2$, fructose 6-(disodium phosphate)[33]; $K_2$, fructose 6-(dipotassium phosphate)[34]; M2, melezitose II[35]; 1-K, 1-kestose[4]; $Na_3$, trisodium fructose 1,6-bisphosphate[36]; 6K1 and 6K2, 6-kestose[7]; C61 and C62, cycloinulohexaose[5], I, isomaltulose[37]; S, sucrose[2]; P, planteose[38]; L, lactulose trihydrate[39]; St, stachyose[7]; R, raffinose[40]; M1, melezitose I[41]; NaBr, sodium bromide·sucrose[42]; and NaI-1 and NaI-2, sodium iodide·sucrose[43]. The circled points refer to nystose F1, F2, and F3. The distance from the center indicates the puckering amplitude.

a "miniature crystal" model was examined. It consisted of an assembly of six nearest neighbors in the nystose crystal structure, initially generated by these $P2_12_12_1$ symmetry operators: $x, y, z$; $x-1, y, z$; $x+1, y, z$; $x+0.5, -y+1.5, 1-z$; $-x+1, y-1.5, -z+0.5$; and $-x+2, y-0.5, -z+0.5$. The water molecules of the crystal structure, located on the surface of the minicrystal, were not included in the calculations. Similar studies have maintained space group symmetry or unit cell dimensions, or held the outer molecules fixed during optimization of the central molecule. In our work, however, there were no

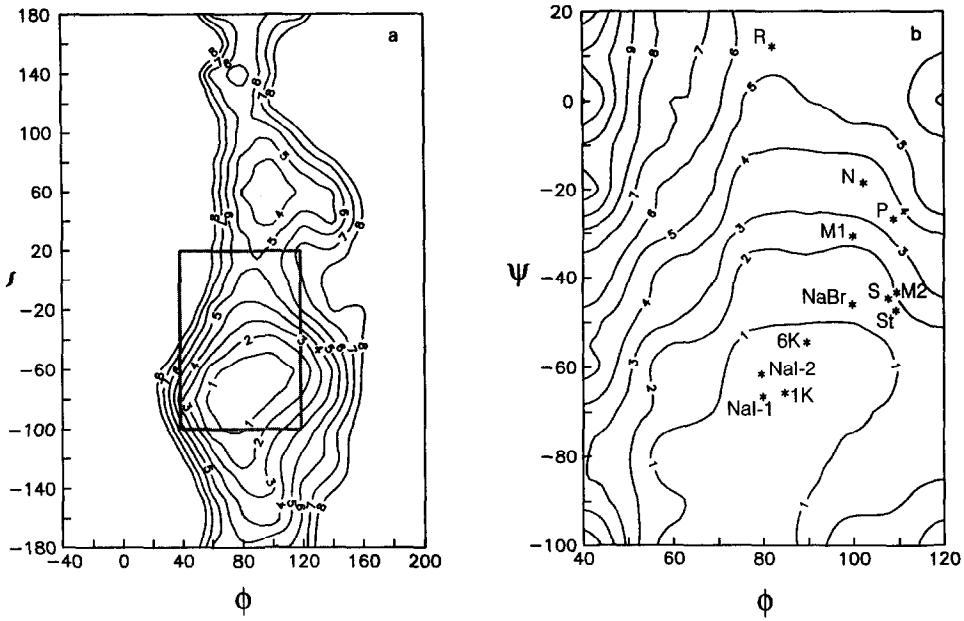


Fig. 2. MM3 energies for isolated sucrose, increments of 1 kcal·mol$^{-1}$. (a) Area covered by four starting models; the rectangle shows the area mapped in b. (b) Area covered by 16 starting geometries and the conformations of the sucrose linkages in the crystal structures of nystose and related oligosaccharides. See the key to Fig. 1 for interpretation of the codes.

restrictions of atomic movement during optimization of the model minicrystal. The minicrystal method was subsequently applied to other carbohydrates[17].

## RESULTS AND DISCUSSION

*Furanose ring conformations.*—The three fructosyl rings of the nystose crystal structure have puckerings of $\Phi = 269$, 304, and 258°. Of these, rings 1 and 3 would fall within the lowest 0.5 kcal · mol$^{-1}$ contour on the MMP2(85) map[8], but ring 2, with a $^4T_5$ shape, is placed 2.5 kcal above the minimum. In the MM3 calculations shown in Fig. 1, all nystosyl conformations lie on or within the 1 kcal · mol$^{-1}$ contour.

The MM3 map, with a larger area within the 1 kcal · mol$^{-1}$ contour, appears to be somewhat more consistent with the crystal structures than the MMP2(85) work. In addition to having lower energies in several cases, the MM3 crystal structures are distributed evenly over the low energy area. MM3 may also better accommodate solution behavior. Recent optical rotation studies of aqueous solutions of methyl β-D-fructofuranoside and sucrose suggest $^4T_5$ shapes[18].

*The sucrose moiety.*—Recent studies suggest that the interresidue linkage of sucrose is flexible[19,20], particularly with respect to rotation about the pseudo-equa-

torial O-1–C-2′ bond. The ranges of values for torsion angles of various sucrosyl linkages in oligosaccharide crystal structures also support this view. Further illustration is given in Figs. 2a and 2b, showing the MM3 energy surface for the isolated sucrose molecule, and Figs. 3a and 3b, showing the PFOS maps for the isolated sucrose linkage. The sucrose linkage in crystalline nystose falls in the gap between raffinose[21] and the cluster of other crystalline examples shown on these energy maps. Its position as an intermediate structure suggests that there is a continuum of likely structures over the range of $\psi = -70$ to 10°, rather than a separate minimum near the raffinose structure. Fig. 3a is almost identical to a map (not shown) that included the remainder of the nystose molecule, with fixed crystallographic geometry for everything but the sucrose linkage bonds. This essential identity suggests that the conformation of the sucrose component of the model is not affected very much by the remainder of the molecule. This is consistent with the extended conformation found in the crystal structure and the absence of interresidue hydrogen bonds.

There are, however, substantial differences between the PFOS and the MM3 maps. The low-energy areas on the PFOS maps are small, typical of rigid-residue methods[22]. Mainly because the starting geometry was from the nystose crystal structure, the crystallographically observed conformation is only 0.8 kcal · mol$^{-1}$ above the minimum. Other structures, 1-kestose and raffinose, have energies of 5 kcal · mol$^{-1}$ or more on this PFOS map, which differs significantly from a PFOS map based on a sucrose moiety optimized with MM2(85)[19]. It also differs strongly from the sucrose map published in the crystallographic study of 6-kestose[6]. That rigid-residue map puts the raffinose geometry on a 100 kcal · mol$^{-1}$ contour. As concluded in that work, such maps are clearly sensitive to starting geometry.

On the MM3 map for sucrose (Fig. 2), derived independently of the crystal structure coordinates, the nystose linkage conformation is 3.5 kcal · mol$^{-1}$ above the minimum, while the most distant outlier, raffinose, is higher than 5 kcal · mol$^{-1}$. Thus, the MM3 result is in agreement with two other relaxed-residue studies that show substantial distortion energy (8 and 9 kcal · mol$^{-1}$) for the raffinose geometry[10,11]. The MM3 energies for raffinose, nystose, and planteose are all higher than found in a wide range of maltosyl moieties[23,24]. There has been little study of the

Fig. 3. PFOS $\phi$, $\psi$ maps for the linkages in nystose. Plus signs (+) indicate the energy minima, and asterisks (*) show the conformations in nystose crystals. Contours are at 1, 2, 5, and 11 kcal·mol$^{-1}$. (a) The isolated sucrose map and (b) Magnification of the low-energy region. In both, $\phi$ is the torsion angle O-5–C-1–O-1–C-2′ and $\psi$ is C-1–O-1–C-2′–O-2′. (c) Map for the isolated F1–F2 inulobiose linkage, with the O-2′–C-2′–C-1′–O-1′ torsion angle, $\chi$, left at the observed value of −63.3°. (d) Map for the F1–F2 linkage as a part of the nystose molecule, otherwise the same as in (c). In both, $\phi$ is the torsion angle O-2″–C-2″–O-1′–C-1′ and $\psi$ is C-2″–O-1′–C-1′–C-2′. (e) Map for the isolated F2–F3 inulobiose linkage, with the O-2″–C-2″–C-1″–O-1″ torsion angle, $\chi$, left at the observed value of −175.9°. (f) Map for the F2–F3 linkage as a part of the nystose molecule, otherwise the same as in (e). In both, $\phi$ is the torsion angle O-2″–C-2″–O-1′–C-1′ and $\psi$ is C-2″–O-1′–C-1′–C-2′.

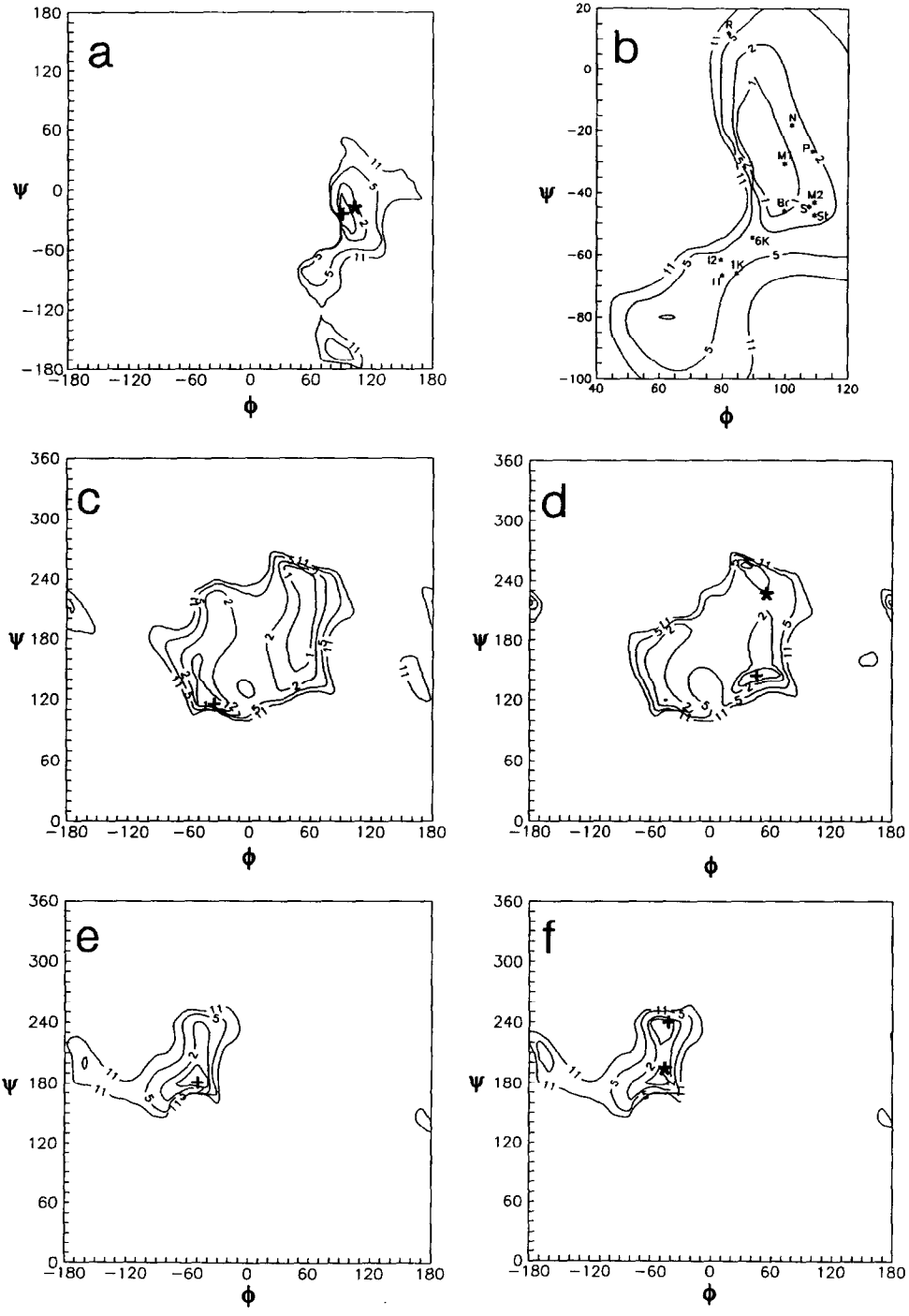
a
b
c
d
e
f
ψ
ϕ
R
N
M1
P2
M2
Br
Sy
St
*6K
I2*
1K

energies of molecules such as sucrose and trehalose having adjacent anomeric centers and thus overlapping exoanomeric effects. Therefore, molecular mechanics calculations for such molecules may not be well founded. An ab initio study of a tetrahydropyran–tetrahydrofuran analogue of sucrose suggests that the MM3 energies of sucrose linkages in nystose and raffinose are overestimated by several kcal · mol$^{-1}$ (ref. 25).

*The inulobiose residues.*—Crystallographic data show a tendency for the central bond in three-bond linkages to adopt a torsion angle of 180° (ref. 12). Nystose deviates most from the rule, at $\psi_{1-2} = -133°$. PFOS maps for the fructose–fructose linkages are shown in Figs. 3c–f. The substantial difference between Figs. 3c and 3e is due to the different orientations about the C-2′–C-1′ and C-2″–C-1″ bonds and the orientation of the C-6‴–O-6‴ primary alcohol group on F3, which restricts the freedom of rotation about the C-2‴–O-1″ bond.

The differences between the isolated inulobiose linkage maps (Figs. 3c and 3e) and the maps in which the entire nystose molecule was present (Figs. 3d and 3f) are subtle but important, at least for the central, F1–F2 linkage. There (compare Figs. 3c and 3d), the positions of the overall minima depend on the presence of the adjacent residues. The crystal conformation of the F1–F2 linkage has a calculated energy of 1.6 kcal · mol$^{-1}$ above the minimum; it sits on a saddle point midway between two minima. For the F2–F3 linkage, the conformation found experimentally falls near the minimum on the PFOS $\phi$, $\psi$ map for inulobiose (Fig. 3e). On the PFOS map for the same linkage in nystose, the observed form is near an almost equienergetic second minimum.

On the $\psi$, $\chi$ surfaces, the presence of the entire nystose molecule places a sharp barrier to values of $\chi = 100°$ for the F1–F2 linkage, but the F2–F3 linkage is not affected very much. All $\psi$, $\chi$ maps had deep energy wells at the three staggered values of $\chi$. Curiously, the crystallographically determined value of $\chi$ for the F1–F2 linkage falls in the lowest energy well for the isolated inulobiose model, but has an energy 2.5 kcal above the minimum when plotted on the PFOS map generated with the entire nystose molecule. There, the overall minimum is 120° (in $\psi$) away from the crystal conformation. The observed $\chi$ value for the F2–F3 linkage falls within 40° and 1 kcal · mol$^{-1}$ of the predicted minimum.

We may also compare the present results with recently published flexible-residue modeling studies of the inulobiose linkage that used MMP2(85)[12] and MM2(87)[13]. The MMP2(85) work on an isolated inulobiose molecule showed (after bringing the torsion angle definitions into conformity with the present work) that the energy was lowest when $\phi$ (O-2″–C-2″–O-1′–C-1′) = −60° and $\chi$ (O-2′–C-2′–C-1′–O-1′) = +60°. Subsequent studies of 1-kestose with MM2(87)[13] showed that the presence of a glucose ring raised the energy of inulobiose conformations with $\chi = +60°$; conformations near $\chi = 180°$ were then preferred, in agreement with the crystal structure. Although the crystallographic $\psi_{1-2}$ value of −133° for nystose is closer to the preferred staggered value of 180° than it is to other staggered values, examination of the MMP2(85) inulobiose map shows that its

TABLE I

Comparison of crystallographic and modeling studies of the inulobiose linkage

| Torsion angle | Values found (deg) | | | | | | |
|---|---|---|---|---|---|---|---|
| | Crystal nystose | Crystal kestose[4] | MM2(87) kestose[13] | PFOS $\phi, \psi$ inulobiose | PFOS $\phi, \psi$ nystose | PFOS $\phi, \chi$ inulobiose | PFOS $\phi, \chi$ nystose |
| $\chi_{1-2}$ | −63 | 179 | 175 | [a] | [a] | −60 | 55 |
| $\psi_{1-2}$ | −133 | −170 | 177 | 120 | 145 | −175 | −175 |
| $\phi_{1-2}$ | 56 | −41 | −70 | −40 | 55 | [a] | [a] |
| $\chi_{2-3}$ | −176 | 179 [b] | 175 [b] | [a] | [a] | −60 | 45 |
| $\psi_{2-3}$ | −165 | −170 [b] | 177 [b] | 180 | 240 | 165 | 165 |
| $\phi_{2-3}$ | −47 | −41 [b] | −70 [b] | −50 | −50 | [a] | [a] |

[a] These torsion angles were held at the crystallographic value while the other two torsion angles of the linkage were varied. [b] The kestose molecule does not have an F2–F3 linkage; these values are the same as for its F1–F2 linkage.

nearly eclipsed conformation is ca. 5 kcal · mol$^{-1}$ higher than the overall minimum in energy.

The results from the PFOS, MM2(87), and crystal studies of the inulobiose linkage are summarized in Table I. The F2–F3 linkage in nystose (−47°, −165°, −176°) conforms fairly well to the inulobiose linkage conformation in the optimal model and the crystal structure of 1-kestose (−70°, 177°, 175° and −41°, −170°, 179, respectively). [An apparent keypunching error in ref 15 gave errors of several degrees in the torsion angles of the XR1 model involving C1′.]

Thus, the predictions of the terminal inulobiose conformations in 1-kestose with the MM2(87) program matched the values observed in 1-kestose and the F2–F3 linkage of nystose as well as might be expected. Even when PFOS found a lower minimum elsewhere, the crystallographic values of the nystose torsion angles in the F2–F3 linkage were in wells of nearly equal energy. The F1–F2 linkage, however, gave poorer agreement. Besides being distorted in $\psi$, the wrong minimum was selected for $\chi$ by both the PFOS and MM2(87) methods. Nor could the inulobiose linkages in either the F2–F3 moiety of nystose or in 1-kestose be used to predict the F1–F2 conformation by extrapolation from the crystal structure. Empirical rules for the conformation of central linkages, such as a principle of tending toward maximum extension, may be needed for the successful prediction of this feature.

*The minicrystal model for nystose.*—When the crystal field arises both from hydrogen bonds and from numerous hydrophobic interactions, substantial distortion is possible for flexible molecules. Distortions as large as 2 kcal · mol$^{-1}$ have been documented for biphenyl crystals[26]. To check for such distortions in nystose, we compared a molecule from its crystal structure optimized in isolation with a molecule optimized as part of a miniature crystal. The results are in Table II. During optimization the changes in torsion angles were less for the minicrystal

TABLE II

Comparisons of torsion angles in the crystal and in models

| Torsion angle | | Values found or calculated (deg) [a] | | |
|---|---|---|---|---|
| | | Crystal structure | Central molecule in crystal model | Isolated model |
| $\phi$ | O-5–C-1–O-1–C-2′ | 102 | 105 (3) | 101 (1) |
| $\psi$ | C-1–O-1–C-2′–O-2′ | −19 [a] | −36 (17) | −54 (35) |
| $\chi_{1-2}$ | O-2′–C-2′–C-1′–O-1′ | −63 | −66 (3) | −63 (0) |
| $\psi_{1-2}$ | C-2′–C-1′–O-1′–C-2″ | −133 [a] | −129 (5) | −157 (24) |
| $\phi_{1-2}$ | C-1′–O-1′–C-2″–O-2″ | 56 | 58 (2) | 62 (6) |
| $\chi_{2-3}$ | O-2″–C-2″–C-1″–O-1″ | −176 | −172 (4) | −165 (11) |
| $\psi_{2-3}$ | C-2″–C-1″–O-1″–C-2‴ | −165 | −165 (0) | −176 (11) |
| $\phi_{2-3}$ | C-1″–O-1″–C-2‴–O-2‴ | −47 | −55 (8) | −58 (11) |

[a] Strain is proposed for these torsion angles, based on the extent of change when they are freely optimized. The numbers in parentheses indicate the absolute values of the changes from the experimental values.

(average 5°) than for the isolated molecule (average 12°). The angles that changed most upon optimization of the isolated molecule, $\psi$ and $\psi_{1-2}$, were those identified above as most distorted. All of these torsion angles refined to conformations near those with minimum energies for the isolated, individual linkages. This indicates that intramolecular forces are not responsible for distortions away from local minima, although they may be responsible for choices of minima other than the global disaccharide minima. The largest torsional change in the minicrystal was for $\psi$ of the sucrose linkage. Thus, even when the crystal field was explicitly included, the crystallographically observed conformation was in conflict with the MM3 parameterization. This again suggests a problem with the parameterization for the overlapped anomeric sequence.

## CONCLUSIONS

In the present work, modeling of furanose rings with MM3 appears to be successful. Similarly, inferences from recent modeling and NMR work that the unusual southern form of the furanose ring found in 1-kestose results from crystal packing were substantiated in the crystal structure of nystose. The modeling work also correctly forecast the terminal inulobiose linkage conformation.

On relaxed energy surfaces, there are often two to four plausible minima. In the case of the furanose rings there are two: a heavily populated Northern minimum and a higher-energy Southern minimum with only one crystal structure present. This is consistent with the Boltzmann distribution. The map for sucrose has three major minima, with all crystal structures found either near the global minimum for the model, or up the sides of the well surrounding the global minimum. In the case of the central inulobiose linkage, two different types of discrepancies were found

when comparing the models with crystalline nystose. There were distortions away from minima, and there were selections of other minima instead of the global minimum. The distortions away from a minimum were examined by explicit inclusion of neighbors in a crystal lattice. If, as was true for the nearly eclipsed $\psi_{1-2}$ torsion, the distorted value was retained, the no fault was assigned to the force field. In the case of $\psi$ for the sucrose linkage, only half of the distortion was retained in the minicrystal. This suggests that the potential function is responsible for the high calculated energy for the experimental conformation. We lack a similar system for explanation of the selection of alternative minima.

Because the conformations of the two inulobiose linkages in the crystal differ, at least one is not at the global minimum of energy for the isolated disaccharide. Assumptions that such global minimum energy shapes can be used to build larger oligomers must therefore be applied cautiously.

ACKNOWLEDGMENTS

The nystose was a gift from Bio-Science, Japan. J.W. Timmermans read the manuscript and sent a draft of his paper on molecular dynamics calculations on inulin oligomers and their NMR spectra[27].

APPENDIX

Compared to its predecessor, MM3 has improved terms for van der Waals forces, hydrogen bonding, anomeric effects, and bond lengths in five-membered rings. Cross terms for torsion stretching are included, as is a pseudo Morse potential for bond stretching[28,29]. The program was obtained from Technical Utilization Corp., Inc., 235 Glen Village Court, Powell, OH 43065. A dielectric constant of 4 was used in all MM3 calculations, and the optimizations continued until the energy changed less than $0.00008n$ kcal $\cdot$ mol$^{-1}$, where $n$ is the number of atoms in the structure.

PFOS (potential for oligosaccharides) energies consist of van der Waals, torsional, exoanomeric-effect, and hydrogen-bond contributions. The van der Waals interactions use a 6–12 potential function, with parameters proposed by Scott and Scheraga[30]. A threefold sinusoidal potential is used for rotation about the glycosidic bonds C-1–O-1, C-2″–O-1″, and C-2″–O-1′, and the intramolecular mechanism proposed by Tvaroška for the exoanomeric effect was added. Thus $E\phi = -1.33\,(1 - \cos\phi) - 0.62\,(1 - \cos 2\phi) + 0.35\,(1 - \cos 3\phi) - 2.92 \sin\phi - 0.76 \sin 2\phi$. The potential for rotation about the C-2′–O-1 bond was $E\psi = 0.5\,(1 - \cos 3\psi)$; there was no similar compensation for the exoanomeric effects here. The potential for rotation about C-2–C-1 bonds was $E\chi = 3.5\,(\cos 3\chi)$. Hydroxyl hydrogens are assumed to rotate to preferred orientations. All E values are in kcal $\cdot$ mol$^{-1}$ (ref. 31).

REFERENCES


1 G.A. Jeffrey and D. Huang, the immediately preceding paper *Carbohydr. Res.*, 247 (1993) 37–50.
2 G.M. Brown and H.A. Levy, *Acta Crystallogr., Sect. B*, 29 (1973) 790–797.
3 J.C. Hanson, L.C. Sieker, and L.H. Jensen, *Acta Crystallogr., Sect. B*, 29 (1973) 797–808.
4 G.A. Jeffrey and Y.J. Park, *Acta Crystallogr., Sect. B*, 28 (1972) 257–267.
5 M. Sawada, T. Tanaka, Y. Takai, T. Hanafusa, T. Taniguchi, M. Kawamura, and T. Uchiyama, *Carbohydr. Res.*, 217 (1991) 7–17.
6 V. Ferretti, V. Bertolasi, G. Gilli, and C.A. Accorsi, *Acta Crystallogr., Sect. C*, 40 (1984) 531–535.
7 G.A. Jeffrey and D. Huang, *Carbohydr. Res.*, 210 (1991) 89–104.
8 A.D. French and V. Tran, *Biopolymers*, 29 (1990) 1599–1611.
9 K. Bock and R.U. Lemieux, *Carbohydr. Res.*, 100 (1982) 63–74.
10 V.H. Tran and J. Brady, *Biopolymers*, 29 (1990) 961–976.
11 F.W. Lichtenthaler, S. Immel, D. Martin, and V. Müller, *Starch*, 44 (1992) 445–456.
12 T.M. Calub, A.L. Waterhouse, and A.D. French, *Carbohydr. Res.*, 207 (1990) 221–235.
13 A.L. Waterhouse, T.M. Calub, and A.D. French, *Carbohydr. Res.*, 217 (1991) 29–42.
14 D. Cremer and J.A. Pople, *J. Am. Chem. Soc.*, 97 (1975) 1354–1358.
15 G.A. Jeffrey and R. Taylor, *Carbohydr. Res.*, 81 (1980) 182–183.
16 A.D. French, V.H. Tran, and S. Pérez, *ACS Symp. Ser.*, 430 (1990) 191–212.
17 A.D. French, D.P. Miller, and A. Aabloo, *Int. J. Biol. Macromol.*, 15 (1993) 30–36.
18 E.S. Stevens and C.A. Duda, *J. Am. Chem. Soc.*, 113 (1991) 8622–8627.
19 C. Hervé du Penhoat, A. Imberty, N. Roques, V. Michon, J. Mentech, G. Descotes, and S. Pérez, *J. Am. Chem. Soc.*, 113 (1991) 3720–3727.
20 L. Poppe and H. van Halbeek, *J. Am. Chem. Soc.*, 114 (1992) 1092–1094.
21 H.M. Berman, *Acta Crystallogr., Sect. B*, 29 (1970) 290–299.
22 A.D. French, *Biopolymers*, 27 (1988) 1519–1525.
23 M.K. Dowd, J. Zeng, A.D. French, and P.J. Reilly, *Carbohydr. Res.*, 230 (1992) 223–244.
24 A.D. French and M.K. Dowd, *Theochem.*, submitted.
25 A.D. French, L. Schäfer, and S.Q. Newton, *Carbohydr. Res.*, 239 (1993) 51–60.
26 N.L. Allinger, F. Li, L. Yan, and J.C. Tai, *J. Comput. Chem.*, 11 (1990) 868–895.
27 J.W. Timmermans, D. de Wit, H. Tournois, B.R. Leeflang, and J.F.G. Vliegenthart, *J. Carbohydr. Chem.*, submitted.
28 N.L. Allinger, Y.H. Yuh, and J.-H. Lii, *J. Am. Chem. Soc.*, 111 (1989) 8551–8566.
29 N.L. Allinger, M. Rahman, and J.-H. Lii, *J. Am. Chem. Soc.*, 112 (1990) 8293–8307.
30 R.A. Scott and H.A. Scheraga, *J. Chem. Phys.*, (1966) 2209–2215.
31 I. Tvaroška and S. Pérez, *Carbohydr. Res.*, 149 (1986) 389–410.
32 T. Tanaguchi, M. Sawada, T. Tanaka, and T. Uchiyama, *Carbohydr. Res.*, 177 (1988) 13–19.
33 T. Lis, *Acta Crystallogr., Sect. C*, 42 (1986) 1745–1748.
34 N. Narendra, T.P. Seshadri, and M.A. Viswamitra, *Acta Crystallogr., Sect. C.*, 41 (1984) 1612–1614.
35 J. Becquart, A. Neuman, and H. Gillier-Pandraud, *Carbohydr. Res.*, 111 (1982) 9–21.
36 S. Cerrini, V.M. Coiro, and D. Lamba, *Carbohydr. Res.*, 147 (1986) 183–190.
37 W. Dreissig and P. Luger, *Acta Crystallogr., Sect. B*, 29 (1973) 514–521.
38 D.C. Rohrer, *Acta Crystallogr., Sect. B*, 28 (1972) 425–433.
39 G.A. Jeffrey, R.A. Wood, P.E. Pfeffer, and K.B. Hicks, *Carbohydr. Res.*, 226 (1992) 29–42.
40 G.A. Jeffrey and D. Huang, *Carbohydr. Res.*, 206 (1990) 173–182.
41 D. Avenel, A. Neuman, and H. Gillier-Pandraud, *Acta Crystallogr., Sect. B*, 32 (1976) 2590–2605.
42 C.A. Accorsi, F. Bellucci, V. Bertolasi, V. Ferretti, and G. Gilli, *Carbohydr. Res.*, 191 (1989) 105–116.
43 C.A. Accorsi, V. Bertolasi, V. Ferretti, and G. Gilli, *Carbohydr. Res.*, 191 (1989) 91–104.